RSC Advances

PAPER

View Article Online
View Journal | View Issue

Cite this: *RSC Adv.*, 2020, **10**, 28148

A water-soluble boronic acid sensor for caffeic acid based on double sites recognition†

Zhancun Bian,[abcd] Guiqian Fang,[abcd] Ran Wang,[abcd] Dongxue Zhan,[bcd] Qingqiang Yao[bcd] and Zhongyu Wu *[bcd]

Received 1st February 2020
Accepted 14th July 2020

DOI: 10.1039/d0ra00980f

rsc.li/rsc-advances

Due to reversibly and covalently binding with Lewis bases and polyols, boronic acid compounds as fluorescent sensors have been widely reported to recognize carbohydrates, ions, hydrogen peroxide, and so on. However, boronic acid sensors for highly selective recognition of caffeic acid rather than catechol or catechol derivatives have not been reported yet. Herein a novel water-soluble sensor **5c** with double recognition sites based on a boronic acid was reported. When 2.3×10^{-4} M of caffeic acid was added, the fluorescence intensity of sensor **5c** decreased by 99.6% *via* inner filter effect (IFE) because its excitation spectrum well overlaps with the absorption spectrum of caffeic acid under neutral condition, while the fluorescence increased or did not change obviously after binding with other analytes including carbohydrates and other catechol derivatives. In addition, the response time to caffeic acid is fast at room temperature, and a high binding constant ($9245.7 \pm 348.3\ M^{-1}$) and low LOD (1.81×10^{-6} M) was calculated. Moreover, determination of caffeic acid content in caffeic acid tablets was studied, and the recovery rate is sufficient. Therefore, sensor **5c** can be used as a potential tool for detecting biologically significant caffeic acid in real samples.

Introduction

As a natural and ubiquitous substance in many people's daily diet, caffeic acid (its structure is shown in Fig. 1) has exhibited excellent pharmacological effects in terms of healthcare and clinical treatment over the past few decades.[1–4] It was reported that 3 μg of caffeic acid can completely inhibit 20 μg phosphodiesterase which is the main composition of snake poison, and 100 μM of caffeic acid can protect venous endothelial cells from the induction of cell apoptosis. In addition, diseases such as upper respiratory infections in children and obesity problems can be prevented by caffeic acid according to the latest researches.[5,6] Caffeic acid preparations in modern medicine including caffeic acid tablets have been widely used clinically for the treatment of hemostasis, leukopenia, and thrombocytopenia *etc.*[7] Moreover, the chemoprotective effect on cancers has been confirmed.[8,9] However, excessive amounts of caffeic acid lead to carcinogenic effects. For instance, studies reported by Hirose and Takesada *et al.* showed that phenolic compounds (including caffeic acid, catechol, sesamol, BHA and 4-methoxyphenol *etc.*) have an additive/synergistic effect on cancer development even at low dose levels compared to control groups.[10] Therefore, quantitative detection of caffeic acid is of great significance for comprehend our daily diet and early diagnosis of diseases.[11]

To date, several analytical methods have been reported to determine caffeic acid, including chromatography (HPLC, GC),[12–15] capillary electrophoresis,[16] voltammetry,[17–19] electrochemical methods,[20–23] and UV-Visible spectrophotometry,[24,25] *etc.* However, there are still some limitations, such as needing expensive instruments, complex sample pretreatment, lengthy analysis time and high cost, *etc.* Therefore, a new platform with simple, sensitive and efficient detection technology is still urgently needed. Fluorescence techniques have been most widely explored due to their high sensitivity, feasibility, and easy-to-operation.[26] However, at present, there are few reports on the detection of caffeic acid utilizing fluorescence sensors, and most of them are detected by quantum dots or enzymatic methods.[23,27–29] For example, a novel caffeic acid fluorescence detection method based on molecularly imprinted polymers (CDs@MIPs) coated with silane functional carbon dots was

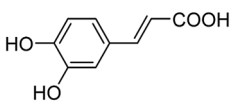

Fig. 1 The structure of caffeic acid.

[a]*School of Medicine and Life Sciences, University of Jinan, Shandong Academy of Medical Sciences, Jinan 250200, Shandong, China*
[b]*Institute of Materia Medica, Shandong First Medical University, Shandong Academy of Medical Sciences, Jinan 250062, Shandong, China. E-mail: wu_med@foxmail.com*
[c]*Key Laboratory for Biotech-Drugs Ministry of Health, Jinan 250062, Shandong, China*
[d]*Key Laboratory for Rare & Uncommon Diseases of Shandong Province, Jinan 250062, Shandong, China*

† Electronic supplementary information (ESI) available. See DOI: 10.1039/d0ra00980f

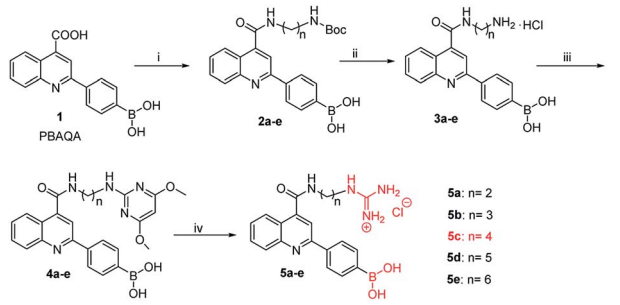

Scheme 1 Synthetic route of sensor **5**: (i) diamine, CH_3OH, DMT-MM, *N*-methylmorpholine, rt, 20 h, **2a**: 75%, **2b**: 81%, **2c**: 73%, **2d**: 79%, **2e**: 78%. (ii) EtOAC, HCl, rt, 18 h, **3a**: 70%, **3b**: 75%, **3c**: 72%, **3d**: 85%, **3e**: 71%. (iii) 2-Chloro-4,6-dimethoxypyrimidine, i-PrOH, NEt_3, reflux, 120 °C, 12 h, **4a**: 35%, **4b**: 52%, **4c**: 47%, **4d**: 46%, **4e**: 48%. (iv) 4 M HCl AcOH/H_2O (1 : 1, v/v), reflux, 100 °C, 10 h, **5a**: 88%, **5b**: 82%, **5c**: 88%, **5d**: 83%, **5e**: 81%.

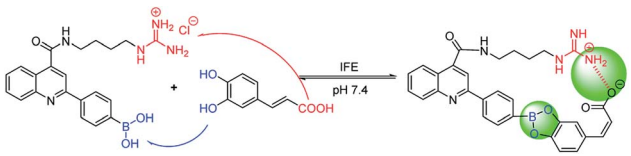

Fig. 2 The process of sensor **5c** recognizes caffeic acid.

proposed by Xu *et al.*[28] Although CD has excellent photoluminescence performance and high biocompatibility, the selectivity of a single carbon dot to the target compound is low, and it needs to be used in combination with other substances, so the synthesis and assembly process is tedious and difficult. Moreover, expensive instruments are needed to characterize the carbon dots. In addition, based on the peroxidase-mimicking activities of the G-quadruplex/hemin DNAzyme, a fluorometric assay platform for fluorescent detection of caffeic acid was designed and reported by Cai *et al.*[23] The experimental operation is complicated and requires dangerous reagents such as H_2SO_4, HCl, HNO_3, and DMSO, *etc.* Moreover, the activity of a DNAzyme is closely related to its configuration, and it is susceptible to environmental influences.

Owing to boronic acid has the unique ability to reversibly bind 1,2- or 1,3-diols in aqueous media, boronic acid-based fluorescent sensors can provide some of the advantages of detecting diols, including high sensitivity and fast response.[30–33] Boronic acid derivatives and their utility in diols sensing including: (1) in clinical practice, some complications such as diabetes and cancer, *etc.* are early diagnosed by detecting certain components in body fluids, saliva or blood;[34] (2) it can be used to test the content of certain ingredients in drug or food products;[35] (3) in the future, fluorescence guided surgery (FGS) can also help doctors determine tumor boundaries and find metastases in the clinic, and guide surgeons to accurately remove tumors. In addition, the structure of 2-aryl-quinoline-4-carboxy derivatives has a large aromatic conjugated system, it has good fluorescent properties.[36,37] Our research group has reported the synthesis of 2-(4-boranephenyl)-quinoline-4-carboxylic acid and its diboronic acid derivatives and studied their fluorescent properties.[30] Sensors have been reported for recognizing sorbitol,[35] ribose,[30] dopamine,[38] levodopa,[36] catechol[37] and Fe^{3+},[39] respectively. Herein, we reported novel water soluble boronic acid compounds with double recognition sites (**5a–e**) for selective detection of caffeic acid based on inner filter effect (IFE).[40,41] As illustrated in Scheme 1, compounds **5** are synthesized through an optimized route and used as fluorescent sensors to detect caffeic acid. Take the representative sensor **5c** for instance, in addition to boronic acid group binding with the *o*-dihydroxy group of caffeic acid, the guanidino group combined with the carboxyl group of caffeic acid to achieve a double recognition effect, which significantly improved the selectivity and affinity, as shown in Fig. 2. The main reason for the interaction between the guanidino group of the sensor **5** and the carboxyl group of caffeic acid is electrostatic attraction. Moreover, the fluorescence of sensor **5c** can be quenched by caffeic acid *via* IFE because its excitation spectrum (328 nm) well overlaps with the absorption spectrum (maximum absorption wavelength at 323 nm) of caffeic acid under neutral condition, as shown in Fig. 3. Due to the simple synthesis, good water solubility, sensitivity, and selectivity, sensor **5c** can be used as a potential tool to detect the caffeic acid content in drug or food products, and even to detect the complications of diabetes early by detecting the caffeic acid content in body fluids.

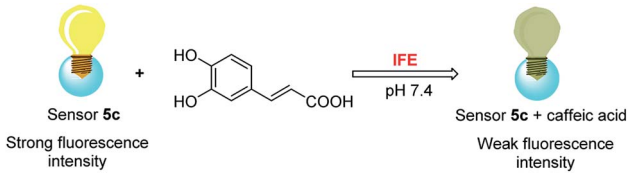

Fig. 3 Mechanism of sensor **5c** recognizes caffeic acid.

Experimental

Materials and methods

All materials for synthesis were commercially available without further purification. All solvents used were of analytical reagent grade and all aqueous solutions were prepared using pure water. The caffeic acid tablets were purchased from Dezhou Deyao Pharmaceutical Co., Ltd. The ^1H NMR spectra and ^{13}C NMR spectra were recorded on a Bruker AM-600 spectrometer (Billerica, MA), and chemical shift (δ) were given in parts per million relative to tetramethylsilane (TMS). High-resolution mass spectrometry (HRMS) spectra were recorded on an Agilent 1290LC-6540 Accurate-Mass Q-TOF by using electrospray ionization (ESI). Chromatographic datas were recorded on a Waters high-performance liquid chromatograph (Waters Corporation, USA), and the separated compounds were collected using a SHIMADZU LC-20AR preparative liquid chromatograph (Shimadzu, Japan). Ultraviolet absorption datas were collected on a HITACHI U-2910 UV-Visible spectrophotometer (Hitachi, Japan). Fluorescence datas were collected on an RF5301PC Fluorescence Spectrophotometer (Shimadzu, Japan).

Synthesis

Owing to compound **1** (PBAQA, 2-(4-boronophenyl)quinoline-4-carboxylic acid) is a known compound and the synthesis process is complicated. Therefore, compound **1** used in our experiments was purchased from a commercial supplier.[36,37,42] As shown in Scheme 1, previously, our research group has reported the synthesis method of compound **3**.[30] In addition, in the synthesis of compound **5**, thiourea trioxide was used as the raw material, and the by-products were more difficult to purify and produced environmentally unfriendly sulfur dioxide after the reaction was complete. So, 2-chloro-4,6-dimethoxypyrimidine was used instead of thiourea trioxide, the reaction was easy to proceed and produced less by-products and waste liquid. Moreover, the experimental operations were relatively simple and the reagents used in the experiment were less toxic.

(4-(4-((2-((*tert*-butoxycarbonyl)amino)ethyl)carbamoyl) quinolin-2-yl)phenyl)boronic acid (2a)

Compound **1** (0.5 g, 1.7×10^{-3} mol) was added to a round bottom flask and methanol (50 mL) was added to dissolve the compound **1**. DMT-MM (0.5 g, 1.9×10^{-3} mol) and *N*-Boc-ethylenediamine (520 μL, 1.9×10^{-3} mol) were then added and completely dissolved by ultrasound, followed by 2 drops of *N*-methylmorpholine. Stirring for 20 h at room temperature, the reaction was stopped, and TLC was used to detect whether the reaction was complete. The reaction solution was concentrated under reduced pressure to at least the amount, and then the reaction solution was slowly added dropwise to 150 mL of ice water with continuous stirring, and a pale yellow precipitate gradually precipitated, followed by filtering. It was then recrystallized from methanol and filtered to give a white powder compound **2a** (0.5549 g, 75%).[30] Compounds **2b**, **2c**, **2d**, and **2e** were synthesized in the same manner as **2a**. The yields of compound **2** as follows: **2a**: 75%, **2b**: 81%, **2c**: 73%, **2d**: 79%, **2e**: 78%, respectively.

(The diamine in reaction (i) includes *N*-Boc-ethylene diamine, *N*-Boc-1,3-propane diamine, *N*-Boc-1,4-butane diamine, *N*-Boc-1,5-diaminopentane, *N*-Boc-1,6-hexane diamine).

(4-(4-((2-aminoethyl)carbamoyl)quinolin-2-yl)phenyl)boronic acid hydrochloride (3a)

The product **2a** (0.5549 g, 1.3×10^{-3} mol) obtained in the previous step was dissolved in a round bottom flask using ethyl acetate (150 mL). Subsequently, 5 mL of hydrochloric acid was slowly added and stirred at room temperature for 18 h. The reaction solution changed from a yellow clear state to a yellow turbid state. After the reaction was completed, the reaction was stopped, and a yellow solid was obtained by suction filtration. It was then washed three times with ethyl acetate and suction filtered, and dried under vacuum to obtain the pale yellow powder compound **3a** (0.3382 g, 70%).[35] Compounds **3b**, **3c**, **3d**, and **3e** were synthesized in the same manner as **3a**. The yields of each compound as follows: **3a**: 70%, **3b**: 75%, **3c**: 72%, **3d**: 85%, **3e**: 71%, respectively.

(4-(4-((2-((4,6-dimethoxypyrimidin-2-yl)amino)ethyl) carbamoyl)quinolin-2-yl)phenyl)boronic acid (4a)

The compound **3a** (0.9034 g, 2.4×10^{-3} mol) was added to a round bottom flask, followed by 12 mL i-PrOH, 1152 μL NEt_3, and the **3a** was completely dissolved by ultrasound. Then, 2-chloro-4, 6-dimethoxypyrimidine (1.0475 g, 6.0×10^{-3} mol) was added and heated to reflux at 120 °C. The reaction was left at this temperature until deemed complete by TLC ($CH_2Cl : CH_3OH = 10 : 1$) analysis, typically 12 h. After the reaction was complete, the reaction was then allowed cool to room temperature and then 10 mL of EtOAc and 5 mL of distilled water were added to the reaction liquid to extract and separate the two phases. The aqueous phase was further washed twice with 5 mL of EtOAc and the two phases were separated. The separated EtOAc phases were combined, washed with a saturated NaCl solution (10 mL), and the two phases were separated. Then anhydrous Na_2SO_4 was used to dry the EtOAc phase, and the precipitate was removed by filtration. The filtrate was reduced by rotary evaporator and concentrated to dry to obtain the off-white powder. Purification was performed by column chromatography ($CH_2Cl : CH_3OH = 100 : 0 \rightarrow 95 : 5$). The collected components were concentrated under reduced pressure to give a white powder compound **4a** (0.3951 g, 35%).[43,44] Compounds **4b**, **4c**, **4d**, and **4e** were synthesized and post processed in the same manner as **4a**. The yields of each compound as follows: **4a**: 35%, **4b**: 52%, **4c**: 47%, **4d**: 46%, **4e**: 48%, respectively.

4a: ^{1}H NMR (600 MHz, CD_3OD) δ (ppm) (Fig. S8, ESI†): 8.94 (d, $J = 5.1$ Hz, 1H), 8.25 (d, $J = 8.2$ Hz, 1H), 8.23–8.15 (m, 2H), 8.16–8.06 (m, 1H), 7.99 (d, $J = 8.1$ Hz, 1H), 7.88–7.75 (m, 1H), 7.69–7.54 (m, 1H), 7.28 (t, $J = 5.3$ Hz, 1H), 5.44–5.31 (m, 1H), 3.79 (s, 4H), 3.57 (t, $J = 7.0$ Hz, 2H), 3.34 (s, 3H), 2.56–2.45 (m, 1H). HRMS (ESI) (Fig. S9, ESI†): calculated for $C_{24}H_{25}BN_5O_5^+$ $[M + H]^+$: 474.1943 found 474.1937.

4c: HRMS (ESI) (Fig. S10, ESI†): calculated for $C_{26}H_{28}BN_5O_5^+$ $[M + H]^+$: 502.2256 found 502.2271.

Synthesis of compound 5

(4-(4-((2-guanidinoethyl)carbamoyl)quinolin-2-yl)phenyl) boronic acid hydrochloride (5a). The synthesized compound **4a** (0.3949 g, 0.8×10^{-3} mol) was added to the round-bottom flask, followed by 3.5 mL AcOH, 3.5 mL distilled water and 18 mL 4 M HCl were added in this order, and **4a** was completely dissolved by ultrasound and refluxed at 100 °C for 10 h. After the reaction was detected to be complete by TLC, the reaction was stopped and cooled to room temperature. 20 mL of EtOAc was added to the reaction solution, and the two phases were separated by extraction. The aqueous phase was further washed with EtOAc (2×20 mL), and then the aqueous phase was washed with 10 mL $CH_2Cl_2 : CH_3OH = 8.5 : 1.5$ and the two phases were separated. The separated aqueous phase was concentrated to dryness under reduced pressure by a rotary evaporator, and a yellow oily solid was obtained after vacuum drying. The previously obtained yellow oily solid was separated by liquid preparative chromatography (chromatographic methanol with a mobile phase of 35%), and the collected components were concentrated under reduced pressure and dried under vacuum

to obtain a yellow powder compound **5a** (0.2921 g, 88%).[43,45] ^{1}H NMR (600 MHz, DMSO) δ (ppm) (Fig. S11, ESI†): 9.15 (t, J = 5.5 Hz, 1H), 8.35 (d, J = 7.4 Hz, 2H), 8.25 (d, J = 8.3 Hz, 1H), 8.19 (d, J = 8.3 Hz, 1H), 8.07 (t, J = 5.9 Hz, 1H), 8.01 (d, J = 8.2 Hz, 1H), 7.88–7.84 (m, 1H), 7.70–7.66 (m, 1H), 3.53 (dd, J = 11.4, 5.6 Hz, 2H), 3.46 (dd, J = 11.5, 5.7 Hz, 2H). ^{13}C NMR (151 MHz, DMSO) δ (ppm) (Fig. S12, ESI†): δ 168.25, 158.58, 157.04, 148.62, 144.47, 140.22, 137.37, 135.95, 131.77, 130.2, 128.65, 127.77, 127.48, 126.87, 124.72, 118.57, 100.00, 41.45, 39.92. HRMS (ESI) (Fig. S13, ESI†): calculated for $C_{19}H_{21}BN_5O_3^+$ $[M + H]^+$: 378.1732 found 378.1715.

(4-(4-((3-guanidinopropyl)carbamoyl)quinolin-2-yl)phenyl) boronic acid hydrochloride (5b). The compound synthesis operation was the same as that of **5a**. Compound **4b** (0.1901 g, 0.39 × 10^{-3} mol) was used instead of **4a** to obtain a yellow powder compound **5b** (0.1360 g, 82%). ^{1}H NMR (600 MHz, MeOD) δ (ppm) (Fig. S14, ESI†): 8.25–8.12 (m, 4H), 8.11 (s, 1H), 7.95 (s, 1H), 7.90–7.75 (m, 2H), 7.71–7.64 (m, 1H), 3.60 (t, J = 6.9 Hz, 2H), 3.36 (t, J = 6.9 Hz, 2H), 1.99 (p, J = 6.9 Hz, 2H). ^{13}C NMR (151 MHz, MeOD) δ (ppm) (Fig. S15, ESI†): δ 168.58, 157.42, 157.19, 147.42, 143.83, 139.23, 134.19, 130.66, 127.87, 127.36–127.23, 126.58, 125.01, 123.57, 117.31, 38.74, 36.73, 28.46. HRMS (ESI) (Fig. S16, ESI†): calculated for $C_{20}H_{23}BN_5O_3^+$ $[M + H]^+$: 392.1888 found 392.1850.

(4-(4-((4-guanidinobutyl)carbamoyl)quinolin-2-yl)phenyl) boronic acid hydrochloride (5c). The compound synthesis operation was the same as that of **5a**. Compound **4c** (0.5679 g, 1.1 × 10^{-3} mol) was used instead of **4a** to obtain a yellow powder compound **5c** (0.4258 g, 88%). ^{1}H NMR (600 MHz, DMSO) δ (ppm) (Fig. S17, ESI†): 9.02 (t, J = 5.5 Hz, 1H), 8.30 (d, J = 8.2 Hz, 2H), 8.20 (d, J = 8.7 Hz, 3H), 8.01 (d, J = 8.1 Hz, 2H), 7.87 (dd, J = 13.2, 6.7 Hz, 2H), 7.69 (t, J = 7.7 Hz, 1H), 3.43–3.38 (m, 2H), 3.22–3.16 (m, 2H), 1.70–1.57 (m, 4H). ^{13}C NMR (151 MHz, MeOD) δ (ppm) (Fig. S18, ESIb†): δ 167.21, 162.26, 209.14–136.26, 134.41, 134.34, 135.29–127.72, 127.19, 126.23, 66.08. HRMS (ESI) (Fig. S19, ESI†): calculated for $C_{21}H_{25}BN_5O_3^+$ $[M + H]^+$: 406.2045 found 406.2087.

(4-(4-((5-guanidinopentyl)carbamoyl)quinolin-2-yl)phenyl) boronic acid hydrochloride (5d). The compound synthesis operation was the same as that of **5a**. Compound **4d** (0.2100 g, 0.41 × 10^{-3} mol) was used instead of **4a** to obtain a yellow powder compound **5d** (0.1556 g, 83%). ^{1}H NMR (600 MHz, MeOD) δ (ppm) (Fig. S20, ESI†): 8.17 (dd, J = 12.7, 11.8 Hz, 4H), 8.05 (s, 1H), 7.95 (s, 1H), 7.84 (ddd, J = 8.2, 7.0, 1.2 Hz, 2H), 7.69–7.63 (m, 1H), 3.52 (t, J = 7.1 Hz, 2H), 3.22 (t, J = 7.1 Hz, 2H), 1.79–1.72 (m, 2H), 1.69 (dt, J = 15.0, 7.4 Hz, 2H), 1.57–1.49 (m, 2H). ^{13}C NMR (151 MHz, MeOD) δ (ppm) (Fig. S21, ESI†): δ 168.35, 157.16, 147.61, 144.04, 139.44, 132.37, 130.39–130.13, 128.43, 127.36, 126.53, 124.97, 123.60, 117.14, 41.03, 39.37, 28.62, 28.12, 23.74. HRMS (ESI) (Fig. S22, ESI†): calculated for $C_{22}H_{27}BN_5O_3^+$ $[M + H]^+$: 420.2201 found 420.2173.

(4-(4-((6-guanidinohexyl)carbamoyl)quinolin-2-yl)phenyl) boronic acid hydrochloride (5e). The compound synthesis operation was the same as that of **5a**. Compound **4e** (0.1300 g, 0.25 × 10^{-3} mol) was used instead of **4a** to obtain a yellow powder compound **5e** (0.0760 g, 81%). ^{1}H NMR (600 MHz, MeOD) δ (ppm) (Fig. S23, ESI†): 8.19 (ddd, J = 13.1, 7.1, 6.3 Hz, 4H), 8.06 (s, 1H), 7.97 (s, 1H), 7.90–7.75 (m, 2H), 7.67 (ddd, J = 8.2, 7.0, 1.0 Hz, 1H), 3.53 (t, J = 7.2 Hz, 2H), 3.21 (t, J = 7.1 Hz, 2H), 1.82–1.70 (m, 2H), 1.70–1.60 (m, 2H), 1.60–1.45 (m, 4H). ^{13}C NMR (151 MHz, MeOD) δ (ppm) (Fig. S24, ESI†): δ 168.34, 157.22, 157.06, 147.66, 144.02, 134.18, 130.48, 128.51, 127.30, 126.51, 124.94, 123.59, 117.06, 41.04, 39.47, 28.86, 28.44, 26.27, 25.92. HRMS (ESI) (Fig. S25, ESI†): calculated for $C_{23}H_{29}BN_5O_3^+$ $[M + H]^+$: 434.2358 found 434.2325.

Results and discussion

A sensor stock solution (1 × 10^{-3} M) was prepared in water, and 100 μL stock solution was diluted to 10 mL using 0.1 M phosphate buffer (PBS, pH 7.4) to obtain a blank sensor solution (1 × 10^{-5} M). Then, the 0.1 M phosphate buffer solution (pH 7.4) was used to prepare analytes stock solution, such as saccharide analytes stock solution (8 × 10^{-1} M) and acid analytes stock solution (8 × 10^{-3} M). And a blank sensor solution (2 × 10^{-5} M) was mixed with the saccharide and acid analytes stock solution 1 : 1 to prepare saccharide analytes stock solution (4 × 10^{-1} M) and acid analytes stock solution (4 × 10^{-3} M), respectively. By reducing different volumes of saccharide or acid analytes sensor stock solutions and adding different volumes of sensor stock solutions (1 × 10^{-5} M), obtaining 1 mL sensor (1 × 10^{-5} M) with different analyte concentrations (0 to 4 × 10^{-1} M or 4 × 10^{-3} M), and the fluorescence spectrum was recorded while testing. The UV-Vis absorption spectrum of the sensor **1** was recorded in DMSO/PBS (1 : 99, v/v) and the sensor **5c** was recorded in PBS (Fig. S1, ESI†). The excitation wavelength of the boronic acid sensor **5c** was set to 328 nm (slit: 5 nm/5 nm), while the maximum fluorescence emission intensity of the boronic acid sensor **5c** was approximately 395 nm, as shown in Fig. S4 (ESI†).

Fluorescence properties

To examine the fluorescence binding affinities of compounds **5a–e** and various analytes, we conducted a series of fluorescence activity studies. When the concentration of analytes added is 6.7 × 10^{-4} M. We found that the sensor has a significant fluorescence response to catechol compounds. Especially, sensor **5c** is found to have the highest binding constant for caffeic acid

Table 1 The key information of sensor **1** and **5** combining with caffeic acid (6.7 × 10^{-4} M)

Sensors	$(I - I_0)/I_0$	LOD[a] (M)	K_{eq}[b] (M^{-1})
1	0.26	1.74 × 10^{-4}	1179.7 ± 149.0
5a	0.96	5.11 × 10^{-6}	7118.9 ± 281.1
5b	0.97	2.25 × 10^{-6}	7839.4 ± 295.9
5c	0.98	1.81 × 10^{-6}	9245.7 ± 348.3
5d	0.95	3.85 × 10^{-6}	5203.6 ± 92.1
5e	0.97	5.53 × 10^{-6}	5738.6 ± 167.3

[a] The value was calculated by $3\delta/S$ ($R^2 > 0.99$). [b] The value was calculated by Benesi–Hildebrand equation based on three times of measurement ($R^2 > 0.99$).

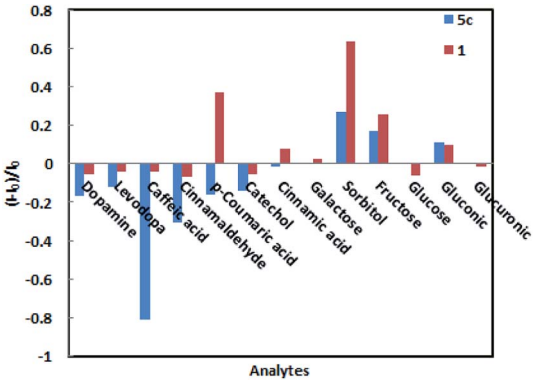

Fig. 4 Relative fluorescence intensity of sensor **1** and **5c** to a low concentration of analytes (2.3×10^{-4} M) in phosphate buffer at pH 7.4.

($9245.7 \pm 348.3\ M^{-1}$) among the several sensors tested, and the lowest detection limit (LOD) (1.81×10^{-6} M) at pH 7.4, as shown in Fig. S4 (ESI†). Compared with sensor **5**, the binding constant of the sensor **1** is significantly lower, as shown in Table 1. The probable reason is that the sensor **1** has only one recognition site (boronic acid group), while the sensor **5** has two recognition sites (boronic acid group and guanidine group). Therefore, the binding affinity and selectivity of the sensor **5** are significantly higher than that of sensor **1**. Moreover, the binding constant of the sensor **5c** and caffeic acid is higher than that of the sensors **5a**, **5b**, **5d**, and **5e**, possibly due to the sensor **5c** has a linker of an appropriate length and rigidity, which provides the suitable spatial structure for the sensor **5c**.

When low concentrations of different analytes (2.3×10^{-4} M) are added, the amplitude changes in the fluorescence intensity of sensors **1** and **5c** as shown in Fig. 4. Among them, caffeic acid causes the largest changes in various analytes. The fluorescence intensity of sensor **5c** decreased by 99.6% after combined with low-concentration caffeic acid (2.3×10^{-4} M), and its fluorescence is almost completely quenched, followed by dopamine, catechol, and levodopa. However, its fluorescence intensity increased or did not change obviously after binding with other analytes. Especially, when combined with glucose, the fluorescence intensity is virtually zero, indicating that sensor **5c** cannot recognize glucose. Although the fluorescence intensity of boronic acid sensor **1** decreased by 93.7% after combined with caffeic acid, the binding constant is low and the linearity is poor. In addition, except sorbitol, the fluorescence intensity of sensor **1** is not change obviously after binding with other analytes. From the above, sensor **5c** can selectively recognize low concentrations of caffeic acid in a phosphate buffer solution with a pH of 7.4.

These studies indicate that if there is no hydroxyl group or only one hydroxyl group in the structure of the analytes, such as cinnamaldehyde, *p*-coumaric acid and cinnamic acid, the

Table 2 Binding constants (K_a) of sensor **5c** with different analytes[a]

Analytes	K_a (M^{-1})
Catechol	795.6 ± 4.2
Dopamine	893.3 ± 16.3
Levodopa	746.6 ± 22.1
Caffeic acid	9245.7 ± 348.3
Galactose	15.6 ± 0.9
Sorbitol	347.1 ± 2.4
Fructose	404.4 ± 4.5
Glucose	—
Gluconic	135.9 ± 1.0
Glucuronic	—

[a] K_a the value was calculated by Benesi–Hildebrand equation based on three times of measurement ($R^2 > 0.99$).

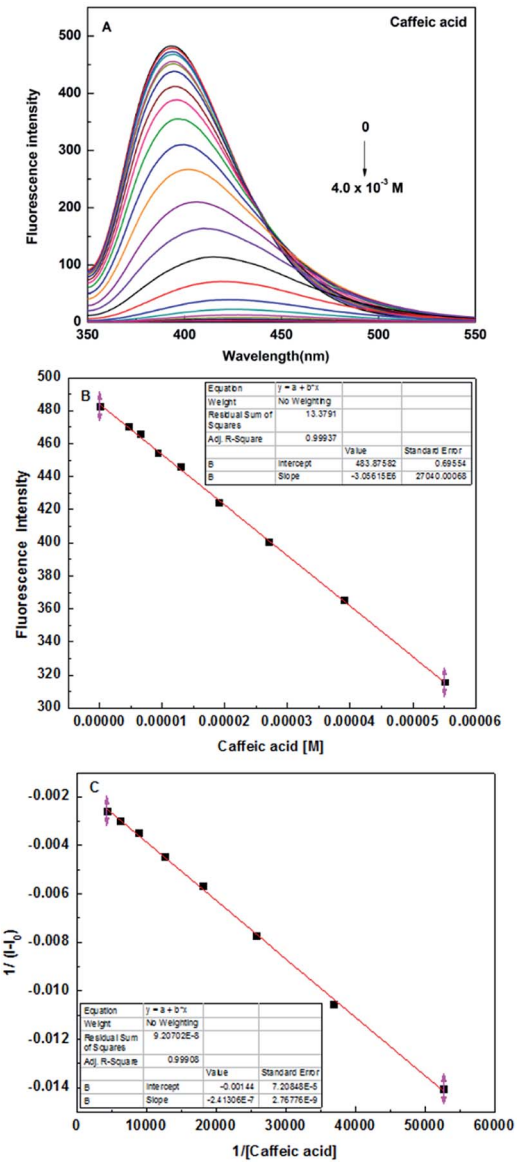

Fig. 5 (A) Fluorescence spectra of sensor **5c** (1×10^{-5} M) in the presence of different concentrations of caffeic acid in PBS (pH 7.4) solution, at room temperature; (B) the photograph of sensor **5c** linear range; (C) Benesi–Hildebrand plot of sensor **5c** $1/(I - I_0)$ *versus* 1/[Caffeic acid].

fluorescence intensity of the sensor **5c** does almost unchanged. Moreover, when it contains only *o*-dihydroxy group and no carboxyl group or aldehyde group, such as catechol, the fluorescence intensity of the sensor hardly changes. Therefore, when the boronic acid group of the sensor **5c** is combined with the *o*-dihydroxy group of the analytes, the guanidine group is combined with the carboxyl group or the aldehyde group, and the fluorescence intensity changes significantly when the two groups work synergistically.

In addition, under the same conditions, we also studied the optimal binding ability of sensor **5c** to other analytes, where the fluorescence intensity reached saturation at the added concentration, as shown in Table 2. When the concentration of the added saccharide analytes is increased from 0 to 4×10^{-1} M, the fluorescence of sorbitol and fructose increased and reached saturation, but the fluorescence intensity of glucose is almost zero. However, when the concentration of the added acid analytes is increased from 0 to 4×10^{-3} M, except for glucuronic acid, the fluorescence is almost quenched after the sensor **5c** is combined with the acid analytes.[37] Especially, the sensor **5c** has the strongest binding capacity to caffeic acid, and its fluorescence is completely quenched (Fig. S7, ESI†).

In order to further study the binding ability of sensor **5c** to caffeic acid, the fluorescence titration experiment was performed. When the concentration of caffeic acid increased from 0 to 4×10^{-3} M, the fluorescence intensity of sensor **5c** decreased by 99.6%, which is almost completely quenched, as shown in Fig. 5A. And the fluorescence titration of sensor **5c** with other analytes is shown in Fig. S7 (ESI†). In addition, when the added caffeic acid concentration is in the range of 4.6×10^{-6} M to 5.5×10^{-5} M, there is a good linear relationship between the fluorescence intensity of the sensor **5c** and the caffeic acid concentration, and the correlation coefficient is $R^2 = 0.99937$, as shown in Fig. 5B. Therefore, the linear regression equation can be determined from Fig. 5B as $I = -3\,056\,150c + 483.87582$, where c is the concentration of caffeic acid and I is the maximum emission fluorescence intensity at 395 nm. Then the LOD is calculated as 1.81×10^{-6} M by the following equation.[46,47]

$$\mathrm{LOD} = 3\delta/S$$

where δ is the standard deviation of the 5 times blank signal of the sensor, and S is the slope of the calibration curve.

In addition, we found that the reciprocal of the decrease in the fluorescence intensity of the sensor **5c** and the reciprocal of the caffeic acid concentration show a good linear relationship, $R^2 = 0.99908$, as shown in Fig. 5C. Benesi–Hildebrand (B–H) equation is a widely used approach for determining the stoichiometry and equilibrium constants of nonbonded interactions, particularly 1 : 1 and 1 : 2 interactions.[48] Therefore, the titrated fluorescence data were processed using the B–H equation and all titrations were performed three times. The titration curve for caffeic acid is fitted and the binding constant (K_a) is 9245.7 ± 348.3 M^{-1} according to the following equation:[30,35,38,49,50]

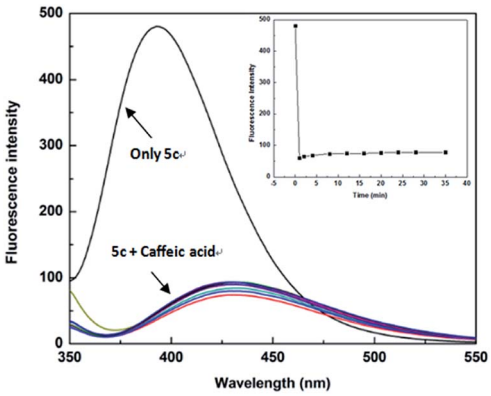

Fig. 6 Fluorescence spectra of sensor **5c** (1.0×10^{-5} M) upon addition of 4.0×10^{-4} M of caffeic acid from 0 to 35 min in PBS (pH 7.4) solution, at room temperature. Inset: plot of the fluorescence intensities at 395 nm over 35 min.

$$\frac{1}{I - I_0} = \frac{1}{I_1 - I_0} + \frac{1}{(I_1 - I_0)K_a[\text{Caffeic acid}]}$$

where I_0 and I_1 are the initial (no caffeic acid) and final fluorescence intensity of the titration curve, I is the observed fluorescence intensity and [Caffeic acid] is the caffeic acid concentration. Using the curve of $(I_1 - I_0)/(I - I_0)$ *versus* 1/[Caffeic acid], K_a can be calculated from the intercept/slope. According to the value of K_a calculated from the B–H equation, it can be found that sensor **5c** has a high binding affinity for caffeic acid. And due to Fig. 5C processed by the B–H equation shows a good linear relationship, $R^2 = 0.99908$, therefore, it can be determined that the binding ratio of sensor **5c** to caffeic acid is 1 : 1.

Response time

The high sensitivity of the sensor is an important aspect of practical applications. In order to be used for the detection of actual samples, it is necessary to explore the sensitivity of the sensor **5c**. Therefore, we performed the response time

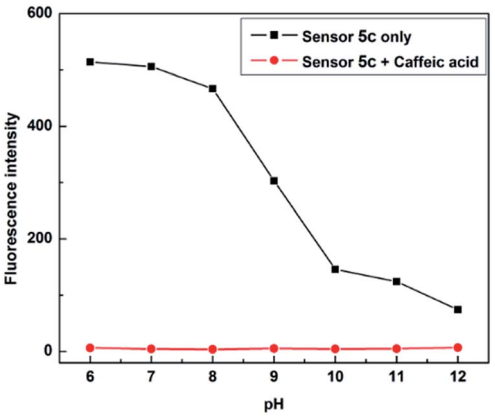

Fig. 7 Fluorescence responses of sensor **5c** (1×10^{-5} M) to caffeic acid (4×10^{-3} M) in phosphate buffer (PBS, 0.1 M) at different pH values.

Table 3 Determination of caffeic acid concentration in caffeic acid tablets

Sample	Caffeic acid added (M)	Caffeic acid found (M)	Recovery%	RSD[a] (%)
Caffeic acid tablets	0	1.29×10^{-5}	—	2.2
	3.0×10^{-5}	4.11×10^{-5}	94	1.3
	3.5×10^{-5}	4.58×10^{-5}	94	1.3
	4.0×10^{-5}	4.99×10^{-5}	93	1.6
	4.5×10^{-5}	5.35×10^{-5}	90	1.2

[a] Relative standard derivation was calculated based on three times of measurements.

Table 4 Comparison of linear range and detection limit between the proposed method and other reported detection methods for caffeic acid

Method	Linear range (M)	LOD (M)	Author
UV-Vis spectrometry	8.8×10^{-4} to 5.6×10^{-1}	0.3×10^{-3}	Zitka,[53] 2011
Liquid chromatography	2.8×10^{-4} to 5.6×10^{-3}	0.11×10^{-3}	Tsai,[54] 1999
Gas chromatography	1.6×10^{-3} to 1.2×10^{-1}	0.53×10^{-3}	Chu,[55] 2001
Voltammetric method	1.0×10^{-5} to 3.5×10^{-1}	2.4×10^{-6}	Karikalan,[11] 2017
Amperometric method	2.0×10^{-3} to 1.0×10^{-2}	0.5×10^{-3}	Demirkol,[56] 2012
Electrochemical sensor	5.0×10^{-4} to 6.0×10^{-2}	0.15×10^{-3}	Leite,[57] 2014
	5.0×10^{-4} to 5.0×10^{-2}	0.05×10^{-3}	Zhang,[26] 2013
Electrochemistry	4.0×10^{-4} to 7.4×10^{-3}	0.29×10^{-3}	Radoi,[58] 2011
	7.4×10^{-4} to 10.5×10^{-3}	0.15×10^{-3}	Diaconu,[59] 2010
Fluorometry	5.0×10^{-4} to 2.0×10^{-1}	0.11×10^{-3}	Xu,[16] 2018
	1.4×10^{-4} to 1.4×10^{-3}	0.06×10^{-3}	Xiang,[27] 2015
	3.7×10^{-3} to 1.1×10^{-1}	1.2×10^{-3}	Fan,[29] 2011
	2.0×10^{-3} to 3.5×10^{-1}	0.2×10^{-3}	Cai,[23] 2016
	4.6×10^{-6} to 5.5×10^{-5}	1.81×10^{-6}	This work

experiment of the reaction system at room temperature (25 °C). The fluorescence of sensor **5c** (1×10^{-5} M) decreased at 395 nm, and its fluorescence intensity is greatly reduced after adding 4.0 $\times 10^{-4}$ M caffeic acid. Fluorescence scans recording requires 0.5 minutes of preparation time. The response time of the test was 0 to 35 minutes, and the recorded time was set to 0, 1, 2, 4, 8, 12, 16, 20, 24, 28, 35 minutes, respectively. Through the response time experiment we found that the fluorescence of the sensor **5c** is greatly reduced to a certain intensity of fluorescence emission, and then it showed very weak fluorescence attenuation over time, as shown in Fig. 6. These results indicate that the response time of the sensor **5c** for caffeic acid is very fast, and real-time detection can be achieved.

pH titration

Due to boronic acid shows different binding forms in acidic and alkaline environments, in order to find the appropriate pH conditions, it is necessary to study the recognition process of sensor **5c** to caffeic acid. A phosphate buffer (PBS, 0.1 M) was first used as the buffered solvent, followed by the solution of hydrochloric acid and sodium hydroxide to adjust the pH. And the pH was adjusted to 6.0, 7.0, 8.0, 9.0, 10.0, 11.0 and 12.0, respectively, as the pH of the sensor **5c** to be studied. Then, different concentrations of caffeic acid were used for fluorescence titration at each pH. The titration curve was made when the concentration of caffeic acid added was 4×10^{-3} M, it could be found that sensor **5c** has a large fluorescence response in the range of pH 6 to 8, as shown in Fig. 7. Considering that the detection sample requires a large fluorescence response, to avoid the trouble of pH adjustment of the buffer solution and to meet the requirements of physiological conditions, therefore, pH 7.4 is a suitable condition for detecting caffeic acid, and all experiments are performed at pH 7.4.

Application of sensor 5c in caffeic acid analysis in real samples

From the above experiments, we know that the sensor **5c** has high selectivity to caffeic acid, so we want to know whether the sensor **5c** can be used for the detection of actual samples, such as caffeic acid in drugs or food products. So, we choose drug caffeic acid tablets for testing, and recovery studies were carried out by spiking the samples with caffeic acid in different concentrations in the range of the linearity. Since the sensor has a good fluorescence response at pH 7.4, a true sample solution to be measured can be prepared with 0.1 M phosphate buffer (pH 7.4) to measure the fluorescence intensity of the actual sample. Using the linear regression equation obtained in Fig. 3B: $I = -3\,056\,150c + 483.87582$. By processing the linear regression equation of fluorescence intensity to convert a series of actual sample concentrations, the equation for calculating the concentration can be converted as follows:

$$C = \frac{I - 483.87582}{(-3\,056\,150)}$$

The recovery and relative standard deviation were calculated by using the calculated concentrations of caffeic acid and spiked caffeic acid. As shown in Table 3, it can be found from the measurement results that caffeic acid has a better recovery rate. Moreover, the active component of caffeic acid tablets is caffeic acid, and there are no pyrocatechol compounds in the pharmaceutical excipients, so the excipients do not interfere with the test results. Therefore, the experimental results show that the sensor **5c** can be applied to the analysis of real samples.[47,51,52]

Comparison with other detection methods

The fluorescence analysis method for detecting caffeic acid is sensitive, fast and does not require complicated sample pretreatment processes, so it has potential application value in real life. As shown in Table 4, the detection methods of caffeic acid that have been reported are compared with the methods used in this paper. The results show that compared to most previously reported methods, our established method provides a better linear range and LOD.

Conclusions

At present, water-soluble boronic acid sensors for selective identification of caffeic acid have not been reported. We synthesized several water-soluble boronic acid sensors using compound **1** as the building block, and detected changes in their fluorescence properties after binding to the various analytes. Among them, when the concentration of the added analytes is 2.3×10^{-4} M, sensor **5c** has the strongest binding capacity to caffeic acid, and its fluorescence intensity is reduced by 99.6%. However, its fluorescence intensity increased or did not change obviously after binding with other analytes. Furthermore, sensor **5c** not only has a very fast response time to caffeic acid under mild conditions (at room temperature) but also has a high binding constant ($9245.7 \pm 348.3\ M^{-1}$) and low LOD (1.81×10^{-6} M) in phosphate buffer (0.1 M, pH 7.4). This indicates that sensor **5c** can selectively recognize caffeic acid *via* fluorescence quenching. In addition, sensor **5c** can be used to detect the caffeic acid content in real samples (such as caffeic acid tablets), and the recovery rate is good. Therefore, the above research shows that the sensor **5c** can be used as a potential tool to detect caffeic acid content in drug or food products and even to diagnose diabetic complications early through caffeic acid detection. Finally, we hope to report that this work will encourage other research groups to discovery more potential boronic acid sensors to recognizing biologically meaningful substances, as well as to develop more promising fluorescence navigation sensors tool for clinical use.

Conflicts of interest

The authors confirm that this article content has no conflict of interest.

Acknowledgements

The authors would like to thank the Innovation Project of the Academy of Medical Sciences for financial support. This work was supported by the National Natural Science Foundation of China (Grant No. 21801158), Shandong Academy of Medical Sciences Foundation (Grant No. 2018-17), and Graduate Instructor Guidance Ability Improvement Project University of Jinan (Grant No. JDYY1804).

Notes and references

1 J. Shen, G. Wang and J. Zuo, *Antiviral Res.*, 2018, **154**, 166–173.
2 X. Zhang, X. He, Q. Chen, J. Lu, S. Rapposelli and R. Pi, *Bioorg. Med. Chem.*, 2018, **26**, 543–550.
3 K. M. M. Espindola, R. G. Ferreira, L. E. M. Narvaez, A. C. R. Silva Rosario, A. H. M. da Silva, A. G. B. Silva, A. P. O. Vieira and M. C. Monteiro, *Front. Oncol.*, 2019, **9**, 1–10.
4 L. P. Pelinson, C. E. Assmann, T. V. Palma, I. B. M. da Cruz, M. M. Pillat, A. Manica, N. Stefanello, G. C. C. Weis, A. de Oliveira Alves, C. M. de Andrade, H. Ulrich, V. M. M. Morsch, M. R. C. Schetinger and M. D. Bagatini, *Mol. Biol. Rep.*, 2019, **46**, 2085–2092.
5 E. Lutfi, P. J. Babin, J. Gutierrez, E. Capilla and I. Navarro, *PLoS One*, 2017, **12**, 1–21.
6 S. Yuksel and S. Akyol, *J. Intercult. Ethnopharmacol.*, 2016, **5**, 308–311.
7 M. Zhang, J. Zhou, L. Wang, B. Li, J. Guo, X. Guan, Q. Han and H. Zhang, *Biol. Pharm. Bull.*, 2014, **37**, 347–354.
8 J. Min, H. Shen, W. Xi, Q. Wang, L. Yin, Y. Zhang, Y. Yu, Q. Yang and Z. N. Wang, *Cell. Physiol. Biochem.*, 2018, **48**, 1433–1442.
9 A. Sharma, M. Kaur, J. K. Katnoria and A. K. Nagpal, *Curr. Med. Chem.*, 2018, **25**, 4740–4757.
10 M. Hirose, Y. Takesada, H. Tanaka, S. Tamano, T. Kato and T. Shirai, *Carcinogenesis*, 1998, **19**, 207–212.
11 N. Karikalan, R. Karthik, S. M. Chen and H. A. Chen, *Sci. Rep.*, 2017, **7**, 1–10.
12 Ş. Karaman, E. Tütem, K. Sözgen Başkan and R. Apak, *Food Chem.*, 2010, **120**, 1201–1209.
13 Z. Bartosova, D. Riman, P. Jakubec, V. Halouzka, J. Hrbac and D. Jirovsky, *Sci. World J.*, 2012, **2012**, 1–6.
14 E. Mesquita and M. Monteiro, *Food Res. Int.*, 2018, **106**, 54–63.
15 H. A. Salman, S. Ramasamy and B. S. Mahmood, *J. Intercult. Ethnopharmacol.*, 2018, **7**, 76–81.
16 Y. Shi, H. Xu, J. Wang, S. Li, Z. Xiong, B. Yan, C. Wang and Y. Du, *Sens. Actuators, B*, 2018, **272**, 135–138.
17 J. Xue, P. T. Lee and R. G. Compton, *Electroanalysis*, 2014, **26**, 1454–1460.
18 Y. Yardim, M. Gulcan and Z. Senturk, *Food Chem.*, 2013, **141**, 1821–1827.
19 S. Ramki, P. Balasubramanian, S. M. Chen, T. W. Chen, T. W. Tseng and B. S. Lou, *Int. J. Electrochem. Sci.*, 2018, **13**, 1241–1249.

20 L. G. Mohtar, P. Aranda, G. A. Messina, M. A. Nazareno, S. V. Pereira, J. Raba and F. A. Bertolino, *Microchem. J.*, 2019, **144**, 13–18.
21 A. Heras, F. Vulcano, J. Garoz-Ruiz, N. Porcelli, F. Terzi, A. Colina, R. Seeber and C. Zanardi, *Sensors*, 2019, **19**, 1–12.
22 H. Mao, Y. Zhang and G. Chen, *Anal. Methods*, 2019, **11**, 303–308.
23 N. Cai, Y. Li, S. Chen and X. Su, *Analyst*, 2016, **141**, 4456–4462.
24 K. Singh and A. Kumar, *Spectrochim. Acta, Part A*, 2019, **211**, 148–153.
25 P. Wongsa, J. Chaiwarith, J. Voranitikul, J. Chaiwongkhajorn, N. Rattanapanone and R. Lanberg, *Chiang Mai J. Sci.*, 2019, **46**, 672–682.
26 J. Song, J. Zhang, F. Lv, Y. Cheng, B. Wang, L. Feng, L. Liu and S. Wang, *Angew. Chem., Int. Ed.*, 2013, **52**, 13020–13023.
27 X. Xiang, J. Shi, F. Huang, M. Zheng and Q. Deng, *Talanta*, 2015, **141**, 182–187.
28 X. Xu, G. Xu, F. Wei, Y. Cen, M. Shi, X. Cheng, Y. Chai, M. Sohail and Q. Hu, *J. Colloid Interface Sci.*, 2018, **529**, 568–574.
29 X. Fan, S. Liu and Y. He, *Colloids Surf., B*, 2011, **88**, 23–30.
30 H. Wang, G. Fang, H. Wang, J. Dou, Z. Bian, Y. Li, H. Chai, Z. Wu and Q. Yao, *New J. Chem.*, 2019, **43**, 4385–4390.
31 X. Zhou, X. Gao, F. Song, C. Wang, F. Chu and S. Wu, *Appl. Surf. Sci.*, 2017, **423**, 810–816.
32 A. L. Chibac, V. Melinte, T. Buruiana and E. C. Buruiana, *Sens. Actuators, B*, 2017, **253**, 987–998.
33 S. K. Munusamy, K. Thirumoorthy, V. P. Muralidharan, U. Balijapalli and S. K. Lyer, *Sens. Actuators, B*, 2017, **244**, 175–181.
34 S. Xu, S. Che, P. Ma, F. Zhang, L. Xu, X. Liu, X. Wang, D. Song and Y. Sun, *Talanta*, 2019, **197**, 548–552.
35 G. Fang, Z. Bian, D. Liu, G. Wu, H. Wang, Z. Wu and Q. Yao, *New J. Chem.*, 2019, **43**, 13802–13809.
36 Z. Wu, X. Yang, W. Xu, B. Wang and H. Fang, *Drug Discoveries Ther.*, 2012, **6**, 238–241.
37 Z. Wu, M. Li, H. Fang and B. Wang, *Bioorg. Med. Chem. Lett.*, 2012, **22**, 7179–7182.
38 H. Wang, G. Fang, K. Wang, Z. Wu and Q. Yao, *Anal. Lett.*, 2018, **52**, 713–727.
39 G. Fang, H. Wang, Z. Bian, M. Guo, Z. Wu and Q. Yao, *RSC Adv.*, 2019, **9**, 20306–20313.
40 L. Han, S. G. Liu, J. Y. Liang, Y. J. Ju, N. B. Li and H. Q. Luo, *J. Hazard. Mater.*, 2019, **362**, 45–52.
41 Z. R. Zhang J, D. Tang, *et al.*, *TrAC, Trends Anal. Chem.*, 2019, **110**, 183–190.
42 H. Y. Chen, J. R. Wei, J. X. Pan, W. Zhang, F. Q. Dang, Z. Q. Zhang and J. Zhang, *Biosens. Bioelectron.*, 2017, **91**, 328–333.
43 J. W. Shaw, L. Barbance, D. H. Grayson and I. Rozas, *Tetrahedron Lett.*, 2015, **56**, 4990–4992.
44 K. B. Suhs T, *Mini-Rev. Org. Chem.*, 2006, **3**, 315–331.
45 D. Hazarika, A. J. Borah and P. Phukan, *Chem. Commun.*, 2019, **55**, 1418–1421.
46 R. Hosseinzadeh, M. Mohadjerani, M. Pooryousef, A. Eslami and S. Emami, *Spectrochim. Acta, Part A*, 2015, **144**, 53–60.
47 R. Hosseinzadeh, M. Mohadjerani and M. Pooryousef, *Anal. Bioanal. Chem.*, 2016, **408**, 1901–1908.
48 R. Wang and Z. Yu, *Acta Phys.-Chim. Sin.*, 2007, **23**, 1353–1359.
49 A. A. Bhatti, M. Oguz, S. Memon and M. Yilmaz, *J. Fluoresc.*, 2017, **27**, 263–270.
50 Y. Dai, K. Yao, J. Fu, K. Xue, L. Yang and K. Xu, *Sens. Actuators, B*, 2017, **251**, 877–884.
51 M. Jamkratoke, G. Tumcharern, T. Tuntulani and B. Tomapatanaget, *J. Fluoresc.*, 2011, **21**, 1179–1187.
52 S. Liu, H. Bai, Q. Sun, W. Zhang and J. Qian, *RSC Adv.*, 2015, **5**, 2837–2843.
53 O. Zitka, J. Sochor, O. Rop, *et al.*, *Molecules*, 2011, **16**, 2914–2936.
54 T. H. Tsai, Y. F. Chen, I. F. Chen, *et al.*, *J. Chromatogr. B: Biomed. Sci. Appl.*, 1999, **729**(2), 119–125.
55 T. Y. Chu, C. H. Chang, Y. C. Liao, *et al.*, *Talanta*, 2001, **54**(6), 1163–1171.
56 D. O. Demirkol, B. Gulsunoglu, C. Ozdemir, *et al.*, *Food Anal. Methods*, 2012, **5**(2), 244–249.
57 W. J. R. Santos, L. T. Kubota and F. R. F. Leite, *Sens. Actuators, B*, 2014, **193**, 238–246.
58 A. Radoi, S. C. Litescu, S. A. V. Eremia, *et al.*, *Microchim. Acta*, 2011, **175**(1–2), 97–104.
59 M. Diaconu, S. C. Litescu and G. L. Radu, *Sens. Actuators, B*, 2010, **145**, 800–806.

